Chemical Abundances in Gaseous Nebulae:
Open problems in Nebular astrophysics
AAA Workshop Series 11, 2019
M. Cardaci, G. Hägele & E. Pérez-Montero, eds.

Poster

Extragalactic Star-forming Regions: a Study of the Physical Properties and Chemical Abundances

Dania Muñoz-Vergara[1,2], Verónica Firpo[2,1], Guillermo Hägele[3,4], Guillermo Bosch[3,4], Mónica Cardaci[3,4], David Sanmartim[2] and Germán Gimeno[2]

[1] *Universidad de La Serena, La Serena, Chile*
[2] *Gemini Observatory, Southern Operations Centre,La Serena, Chile*
[3] *Instituto de Astrofísica de La Plata, CONICET–UNLP, Argentina*
[4] *Facultad de Ciencias Astronómicas y Geofísicas, Universidad Nacional de La Plata, Argentina*

Abstract. Extragalactic star-forming regions are characterized by the large number of young and massive stars that ionize the surrounding gas. These regions can be observed as very luminous spots in the disk of spiral galaxies and as large areas in Blue Compact Dwarf galaxies. We present preliminary results of the study of a sample of star-forming regions in two spiral and one Blue Compact Dwarf galaxies observed with the GMOS/Long-slit configuration on the Gemini-South Telescope. We are presenting a preliminary study of two regions of each galaxy for which we estimated: reddening, electron densities, and electron temperatures by using direct method, temperature relations based on photoionization models, and empirical relations. From the electron temperatures we derived ionic and total chemical abundances of, O, S, N, Ne, Ar and He. In addition we computed star formation rates and the ionization state for all regions.

galaxies: abundances — galaxies: ISM

1. Observation and Data Reduction

We have observed the two spiral galaxies: NGC 5861 and NGC 6070, and the Blue Compact Galaxy: Tol 1924-416A. Data were acquired with the Gemini-South Multi-Object Spectrograph (GMOS) in longslit configuration on April 27, 2007 (program ID: GS-2007A-Q-30, PI: V. Firpo), using the B600 (blue) and R400 (red) gratings to cover a wavelength range ∼3350-9600 Å. Data reduction was performed using the Gemini GMOS IRAF tasks including bias and overscan subtraction, flat fielding, wavelength calibration, and flux calibration. Observing conditions were good, with an average seeing of $0\farcs7$. The R400 grating centered at 7700 Å gives a dispersion of ∼1.3 Å pix^{-1}. The B600 grating centered at 4800 Å gives a dispersion of ∼0.9 Å pix^{-1}. From these observations we have extracted spectroscopic data of 10 star-forming regions, 5 of them located in NGC 5861, 3 in NGC 6070 and the last 2 in Tol 1924-416A. Here we are presenting

preliminary results obtained for two star-forming regions on each galaxy. The whole sample analysis will be presented in Muñoz-Vergara et al. (in prep.).

2. Results

Following the method described by Hägele et al. (2006), we have measured the line and continuum fluxes and estimated the equivalent width (EW) for a good number of emission-lines. Tables 1-3 present the list of emission-lines measured for the two studied regions of the three galaxies (NGC 5861, Tol 1924-416A and NGC 6070, respectively) together with the estimated reddening corrected emission-line intensities, I(λ), in terms of Hβ (assuming F(Hβ)=I(Hβ)=10000), their estimated Equivalent Width (EW), the line intensities percentage error and the Correction Factor f(λ). The reddening constant estimated for each region and its error are also listed in these tables.
The physical conditions of the ionized gas in the star-forming regions were derived following the same methodology as Hägele et al. (2012) and are presented in Table 4. As the [SIII] λ9532 Å could not be measured, its flux was estimated assuming the theoretical value of 2.44× [SIII] λ9069 Å. The electronic density, N_e, was determined from the ratio R_{S2} of the lines [SII] λ6717,6731 Å. The electron temperatures for each ion were derived using the strategy described by Hägele et al. (2012, section 3.2).

Table 1. NGC 5861

		I			II$_{1stComp}$		
λ(Å)	f(λ)	-EW(Å)	I(λ)	Error(%)	-EW(Å)	I(λ)	Error(%)
3727 [OII]dob	0.271	29.11	16112±589	3.7	36.48	21091±592	2.8
4102 Hδ	0.188	8.87	2917±917	31.4	20.00	4730±1575	33.3
4340 Hγ	0.142	32.30	3884±880	22.7	18.00	3829±1504	39.3
4861 Hβ	0.000	50.28	10004±153	1.5	51.00	10006±158	1.6
4959 [OIII]	-0.024	9.02	1917±66	3.4	7.00	1061±188	17.7
5007 [OIII]	-0.035	25.99	5215±32	0.6	16.00	2499±264	10.5
5876 HeI	-0.209	16.73	1622±752	46.4	9.00	844±36	4.3
6300 [OI]	-0.276	2.64	363±18	4.9	2.00	266±57	21.5
6548 [NII]	-0.311	21.05	2474±214	8.7	28.00	3182±310	9.8
6563 Hα	-0.313	251.78	28760±532	1.8	235.00	28899±779	2.7
6584 [NII]	-0.316	61.91	7455±214	2.9	80.00	8828±341	3.9
6678 HeI	-0.329	3.67	365±213	58.4	4.00	301±55	18.2
6717 [SII]	-0.334	34.34	3687±123	3.3	42.00	3936±221	5.6
6731 [SII]	-0.336	22.92	2489±101	4.0	3200	2962±179	6.0
7136 [ArIII]	-0.385	4.46	350±39	11.0	3.00	188±66	35.2
9069 [SIII]	-0.561	18.03	884±41	4.6	17.00	697±64	9.1
c(Hβ)			0.74 ± 0.03			0.94 ± 0.04	
I(Hβ)(erg seg^{-1} cm^{-2})			0.24×10^{-14}			0.17×10^{-14}	

Total chemical abundances derived for the regions considered here are listed in the botom part of Table 4. The total chemical abundances from forbidden lines O, S, Ne and Ar were derived from the measured forbidden emission-lines and using the estimated line temperatures as described by Hägele et al. (2008, 2012). This table includes the adopted value for He^+/H^+ as the average value, weighted by the errors, of the He ionic abundances derived from each He emission-line. In general, all regions are in a low density regime. In both regions of Tol 1924-416 was possible to derive the oxygen abundances with values of ∼0.18 and ∼0.15 times the solar value (12+log(O/H)$_\odot$= 8.69, Allende Prieto et al., 2001) for region I and II, respectively. These results, as well as the derived sulfur abundance, are in good agreement with the obtained by Kehrig et al. (2006), 0.16 times the solar value for the oxygen abundances and 6.08±0.12 for the

Table 2. Tol1924-416A

		I			II		
λ(Å)	f(λ)	-EW(Å)	I(λ)	Error(%)	-EW(Å)	I(λ)	Error(%)
3727 [OII]dob	0.271	87.82	13631±325	2.4	89.45	14065±421	3.0
3868 [NeIII]	0.238	36.64	4208±88	2.1	48.39	4957±169	3.4
3889 HeI+H8	0.233	13.58	1646±72	4.4	23.21	2027±92	4.5
3970 [NeIII]+He	0.215	47.78	3292±168	5.1	30.59	2673±133	5.0
4102 Hδ	0.188	34.26	2700±176	6.5	27.98	2664±437	16.4
4340 Hγ	0.142	74.78	4842±334	6.9	91.75	5263±149	2.8
4363 [OIII]	0.138	11.30	815±50	6.1	14.40	901±90	10.0
4471 HeI	0.106	7.32	471±30	6.4	. . .	. . .	. . .
4861 Hβ	0.000	179.99	10003±228	2.3	178.10	10001±200	2.0
4959 [OIII]	-0.024	281.76	17729±65	0.4	299.76	17691±26	0.1
5007 [OIII]	-0.035	786.43	53184±120	0.2	782.22	52661±106	0.2
5876 HeI	-0.209	25.48	971±19	1.9	34.18	1228±50	4.1
6300 [OI]	-0.276	11.33	363±18	5.1	13.57	548±19	3.5
6312 [SIII]	-0.278	4.43	141±9	6.1	6.04	245±27	11.1
6364 [OI]	. . .	. . .	. . .	. . .	5.80	234±19	8.3
6548 [NII]	-0.311	10.52	319±21	6.5	6.85	272±19	7.1
6563 Hα	-0.313	663.25	28366±186	0.7	767.78	29504±385	1.3
6584 [NII]	-0.316	28.02	854±30	3.5	18.01	727±30	4.1
6678 HeI	-0.329	11.86	311±13	4.3	8.87	302±53	17.7
6717 [SII]	-0.334	46.62	1283±32	2.5	43.76	1666±43	2.6
6731 [SII]	-0.336	32.97	928±29	3.1	30.51	1171±33	2.8
7065 HeI	-0.377	7.60	189±14	7.3	. . .	. . .	. . .
7136 [ArIII]	-0.385	20.23	476±18	3.7	18.48	544±22	4.1
7319 [OII]dob	-0.406	7.47	174±14	8.3	8.13	239±20	8.3
7330 [OII]dob	-0.407	7.69	179±22	12.3	5.89	174±17	9.8
7751 [ArIII]	-0.451	6.31	138±9	6.2	71.00	205±14	7.0
9069 [SIII]	-0.561	41.43	617±26	4.2	38.41	801±34	4.2
c(Hβ)		0.43 ± 0.03				0.25 ± 0.02	
I(Hβ)(erg seg^{-1} cm^{-2})		2.76×10^{-14}				1.60×10^{-14}	

sulfur abundances. The derived oxygen abundance values for NGC 5861 are 0.1 and 0.15 times the solar value in regions I and II$_{1stComp}$, respectively. The value derived for NGC 6070-I is 0.19 times the solar values. These oxygen abundances are consistent with the values estimated for both regions on Tol 1924-416.

Table 3. NGC 6070

				NGC6070			
		I			II		
λ(Å)	f(λ)	-EW(Å)	I(λ)	Error(%)	-EW(Å)	I(λ)	Error(%)
3727 [OII]dob	0.271	53.19	15976±686	4.3	. . .	. . .	. . .
3970 [NeIII]+He	0.215	6.42	1417±153	10.8	. . .	. . .	. . .
4102 Hδ	0.188	30.07	2785±353	12.7	. . .	. . .	. . .
4340 Hγ	0.142	146.72	3672±729	19.8	. . .	. . .	. . .
4861 Hβ	0.000	106.78	10004±145	1.4	57.00	10006±352	3.5
4959 [OIII]	-0.024	68.16	6417±79	1.2	22.00	4592±407	8.9
5007 [OIII]	-0.035	176.47	18617±122	0.7	61.00	12961±591	4.6
5876 HeI	-0.209	17.94	1043±21	2.0	. . .	. . .	. . .
6300 [OI]	-0.276	2.28	169±25	14.7	. . .	. . .	. . .
6548 [NII]	-0.311	30.18	1710±54	3.1	15.00	2022±221	10.9
6563 Hα	-0.313	488.98	28775±586	2.0	261.00	28500±621	2.2
6584 [NII]	-0.316	85.91	4860±128	2.6	45.00	6132±414	6.8
6678 HeI	-0.329	6.40	309±9	2.9	. . .	. . .	. . .
6717 [SII]	-0.334	50.76	2496±68	2.7	34.00	3814±265	7.0
6731 [SII]	-0.336	34.36	1712±50	2.9	22.00	2477±190	7.7
7136 [ArIII]	-0.385	17.77	676±23	3.3	. . .	. . .	. . .
9069 [SIII]	-0.561	63.61	1324±60	4.5	14.00	606±129	21.3
c(Hβ)		0.68 ± 0.03				1.00 ± 0.08	
I(Hβ)(erg seg^{-1} cm^{-2})		0.45×10^{-14}				0.04×10^{-14}	

Table 5 presents the values of Star Formation Rates (SFRs), Hα luminosity (logarithmic scale) for the presented star forming region. For spiral galaxies, SFR and Hα luminosity values are in agreement with values found by Skillman et al. (2003) in 11 spiral galaxies. On the other hand, Tol 1924-416 presents very high values, and they are similar to the values of other BCD galaxies studied by Hopkins et al. (2002); Ramya et al. (2009).

Acknowledgments. DM gratefully acknowledges support from the Gemini Observatory, SoutherOperations Centre, Internship Program and CONICYT-

Table 4. Densities in cm^{-3} and temperatures in 10^4K.

	NGC5861		NGC6070		Tol1924-416	
	I	II$_{1stComp}$	I	II	I	II
n([SII])	10:	80:	10:	20:	25:	10:
T([OIII])	1.0[e]	1.0[e]	1.0[e]	1.0[e]	1.35±0.03	1.42±0.06
T([SIII])	0.87± 0.13[c]	0.87 ± 0.13[c]	0.87[c]	0.87[c]	1.29±0.12	1.47±0.12
T([OII])	1.21±0.04[f]	1.05[f]	1.21[f]	1.15[f]	1.286[d]	1.37[d]
T([SII]	0.98[f]	0.98[f]	0.98[f]	0.94±0.01[f]	1.296[e]	1.208[e]
T([NII])	1.21±0.04[a]	1.05[a]	1.21±0.04[g]	1.15[g]	1.04[b]	1.16[b]
Total and Relative Abundances						
12+log(O/H)	7.67±0.01	7.87±0.03	7.96±0.01	. . .	7.85±0.03	7.79±0.05
12+log(S/H)	6.39±0.11	6.40±0.10	6.53±0.13	. . .	5.87±0.08	5.91±0.07
12+log(Ne/H)	. . .	. . .	. . .	. . .	7.23±0.04	7.24±0.07
12+log(Ar/H)	5.73±0.21	5.50±0.30	5.99±0.18	. . .	5.10±0.05	5.04±0.07
He^+/H^+(adopted)	0.107±0.012	0.062±0.011	0.078±0.002	. . .	0.078±0.011	0.097±0.009

[a]Derived using temperatures predicted by photoinizaton models [b]Derived using temperatures estimated from photoionization models and/or empirical methods. [c]Derived using Hägele et al. (2006) empirical method. [d]Derived using Díaz et al. (2007) empirical method. [e]Assumed temperature=10^4K. [f]Derived using Pérez-Montero & Díaz (2003) method.

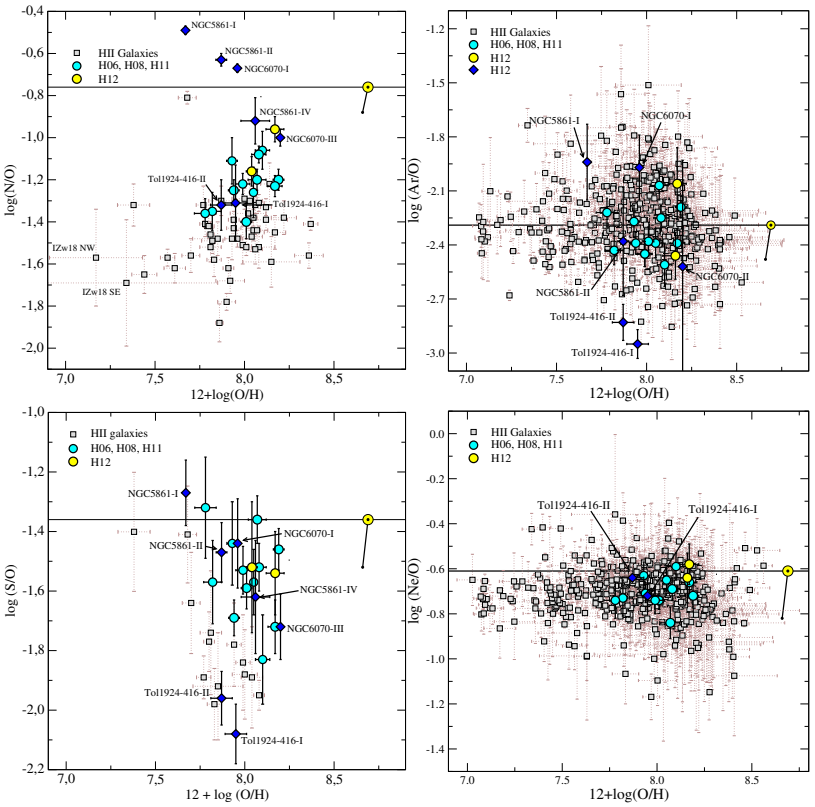

Figure 1. From left to right: N, Ar, S, and Ne relative abundances. The yellow filled sun symbol indicates the solar value. Yellow filled circles are values from Hägele et al. (2012) and cyan filled circles are results from Hägele et al. (2006, 2008, 2011)

PFCHA/Doctorado Nacional/2019-21191543. VF acknowledges support from CONICYT Astronomy Program-2015 Research Fellow GEMINI-CONICYT

Table 5.

Regions	SFR ($\times 10^{-3}$ $M_\odot$ yr^{-1})	log(L(Hα))	err%[L(Hα)]
NGC 5861_I	5.19±0.92	38.82	18
NGC 5861_II$_{1stComp}$	3.69±0.69	38.66	19
NGC 6070_I	10.3±1.93	39.11	19
NGC 6070_II	0.91±0.21	38.06	23
Tol 1924-416_I	103±20.3	40.12	20
Tol 1924-416_II	62.4±12.3	39.90	20

(32RF0002). Based on observations obtained at the Gemini Observatory, which is operated by the Association of Universities for Research in Astronomy, Inc., under a cooperative agreement with the NSF on behalf of the Gemini partnership: the National Science Foundation (United States), the National Research Council (Canada), CONICYT (Chile), Ministerio de Ciencia, Tecnología e Innovación Productiva (Argentina), and Ministério da Ciência, Tecnologia e Inovação (Brazil) and the Korea Astronomy & Space Science Institute (Korea).

References

Allende Prieto C., Lambert D. L., Asplund M., 2001, *ApJL*, **556**, L63
Díaz Á. I., Terlevich E., Castellanos M., Hägele G. F., 2007, *MNRAS*, **382**, 251
Hägele G. F., Díaz Á. I., Terlevich E., Terlevich R., Pérez-Montero E., Cardaci M. V., 2008, *MNRAS*, **383**, 209
Hägele G. F., Firpo V., Bosch G., Díaz Á. I., Morrell N., 2012, *MNRAS*, **422**, 3475
Hägele G. F., García-Benito R., Pérez-Montero E., Díaz Á. I., Cardaci M. V., Firpo V., Terlevich E., Terlevich R., 2011, *MNRAS*, **414**, 272
Hägele G. F., Pérez-Montero E., Díaz Á. I., Terlevich E., Terlevich R., 2006, *MNRAS*, **372**, 293
Hopkins A. M., Schulte-Ladbeck R. E., Drozdovsky I. O., 2002, *AJ*, **124**, 862
Kehrig C., Vílchez J. M., Telles E., Cuisinier F., Pérez-Montero E., 2006, *A&A*, **457**, 477
Pérez-Montero E., Díaz A. I., 2003, *MNRAS*, **346**, 105
Ramya S., Sahu D. K., Prabhu T. P., 2009, *MNRAS*, **396**, 97
Skillman E. D., Côté S., Miller B. W., 2003, *AJ*, **125**, 593